35th Annual International Conference of the IEEE EMBS
Osaka, Japan, 3 - 7 July, 2013

Electromagnetic Tomography via Source-Space-ICA

Yaqub Jonmohamadi, Govinda Poudel, *Member, IEEE,* Carrie Innes, Richard D. Jones, *Senior Member, IEEE*

***Abstract*—We propose a technique, called source-space-ICA to provide spatiotemporal reconstruction of brain sources. First, the weight-vector-normalized minimum variance beamformer is applied to reconstruct the electrical activity of a 3D scanning grid which covers the whole brain. Second, principal component analysis is used to reduce the dimension of the reconstructed signal matrix of the source-space, then independent component analysis (ICA) is applied on the resulting matrix to identify multiple signal sources in the source-space. Third, the demixing weight vectors obtained by ICA for the identified independent components are projected back into the SS to obtain tomographic maps of the sources. Besides localization, the proposed source-space-ICA approach reconstructs the time-course of each source in a single time-series without requiring prior knowledge of location, orientation, and number of sources for a given segment of EEG/MEG. Simulated EEG was used to evaluate the source-space-ICA. The results show that the source-space-ICA approach is able to separate and localize multiple weak sources and is robust to interference from other sources as it identifies the sources based on their statistical independence.**

I. Introduction

ELECTROENCEPHALOGRAPHY (EEG) and magnetoencephalography (MEG) are noninvasive recordings of brain electromagnetic activities with millisecond temporal resolution. The aim of source imaging in EEG and MEG is to spatially localize the neuronal sources and reconstruct their corresponding time-courses. Several methods have been proposed for this, such as dipole fitting, minimum norm spatial filters, minimum variance spatial filters, and variants of these such as adaptive or non-adaptive versions.

Dipole fitting [1] is a popular technique which assumes that a predefined number of dipoles have generated the given EEG/MEG segment. The main limitation of this technique is that the number of sources must be specified in advance. In addition, dipole fitting finds a single point for each brain source and is unable to produce a tomographic map. Minimum-norm based spatial filters, such as the original minimum-norm filter [2] and standardized low resolution electromagnetic tomography (sLORETA) [3] produce a tomographic map for the whole brain for a given MEG/EEG epoch and do not require prior knowledge of the number of brain sources. Minimum-variance spatial filters, such as the adaptive minimum variance (MV) [4–6] beamformer, scan the whole brain voxel by voxel and estimate the power of each voxel for a given epoch to produce a tomographic map. Minimum-variance beamformers have been shown to have a higher spatial resolution than minimum-norm based filters and can reconstruct signal sources with a small signal-to-noise-ratio (SNR) [7].

In the EEG/MEG literature, the source localization problem is mostly focused on strong brain sources (SNR$>$1) while localization of weak sources, such as a SNR=0.25, remains a limitation for current source estimators. This is because source estimators such as minimum-variance and minimum-norm spatial filters calculate the power or magnitude (neural activity index) for each brain voxel to produce a tomographic map of the brain for a given EEG/MEG segment. As a result, only sources with a higher magnitude than the background activity will appear in the map as a source signal.

Independent component analysis (ICA) is a blind source separation technique which aims to separate K mutually statistically independent, zero mean, sources from M linearly combined signal mixtures [8]. In EEG and MEG, ICA is a popular technique for removal of artifacts. In the case of source localization, ICA accompanied with dipole fitting [9] has been applied to localize and reconstruct the time-course of the sources. In this approach, after applying ICA on EEG (sensor-space-ICA), the dipole fitting technique is used to localize the identified sensor-space components in the source-space. One limitation of sensor-space-ICA is that the number of underlying brain sources, K, is much greater than the number of the EEG sensors, M, and sensor-space-ICA is only able to find as many components as the number of the sensors. One way to obtain more components is to apply multiple bandpass filters before ICA. We propose a new technique, called *source-space-ICA* which applies ICA directly in the source-space. The idea of source-space-ICA is to apply spatial filtering to reconstruct the time-courses of the source-space (brain volume) on a 3D scanning grid and then apply ICA to spatiotemporally identify the sources. In this way, the number of identified sources can be greater than the number of sensors. Unlike most source estimators, source-space-ICA relies not only on the magnitude of the sources but also on their statistical independence via ICA. This helps to identify multiple weak, as well as strong, sources. In source-space-ICA, due to spatial filtering, each signal given to ICA is much less mixed with other source signals compared with signals in sensor-space.

We first describe the background equations and then

Manuscript received December 11, 2012.

Y. Jonmohamadi is a PhD student in the Department of Medicine, University of Otago, New Zealand Brain Research Institute, Christchurch, New Zealand (e-mail: jonya247@student.otago.ac.nz).

G. Poudel was with the New Zealand Brain Research Institute, Christchurch, New Zealand and is now with Monash Biomedical Imaging, Monash University, Melbourne, Australia (e-mail: govinda.poudel@monash.edu).

C. R. H. Innes is with the Department of Medical Physics and Bioengineering, Christchurch Hospital, and New Zealand Brain Research Institute, Christchurch, New Zealand (e-mail: carrie.innes@nzbri.org).

R. D. Jones is with the Department of Medical Physics and Bioengineering, Christchurch Hospital, and Department of Medicine, University of Otago, and Department of Electrical & Computer Engineering, University of Canterbury, and New Zealand Brain Research Institute, Christchurch, New Zealand (e-mail: richard.jones@nzbri.org).

describe the experiment to evaluate the performance of the source-space-ICA for source localization of multiple brain sources with different SNRs. Throughout this paper, plain italics indicate scalars, lower-case boldface italics indicate vectors, and upper-case boldface italics indicate matrices.

II. Methods

The measured EEG and MEG signal $\boldsymbol{B}(t) = [\boldsymbol{b}(t_1), \boldsymbol{b}(t_2), ..., \boldsymbol{b}(t_K)]^T$, for K time samples on M electrodes, at time point t is

$$\boldsymbol{b}(t) = \int \boldsymbol{L}(\boldsymbol{r})\boldsymbol{q}(\boldsymbol{r})s(t,\boldsymbol{r})d(\boldsymbol{r}) + \boldsymbol{\eta}(t), \tag{1}$$

and $\boldsymbol{L}(\boldsymbol{r}) = [\boldsymbol{l}_x(\boldsymbol{r}), \boldsymbol{l}_y(\boldsymbol{r}), \boldsymbol{l}_z(\boldsymbol{r})]$ is a $M \times 3$ lead-field matrix which shows the sensitivity of scalp sensors in three orthogonal directions (x,y,z) to the source signal $s(t,\boldsymbol{r})$ located at $\boldsymbol{r} = [r_x, r_y, r_z]^T$ (mm) with a moment of $\boldsymbol{q}(\boldsymbol{r}) = [q_x(\boldsymbol{r}), q_y(\boldsymbol{r}), q_z(\boldsymbol{r})]^T$ (A.m), and $\boldsymbol{\eta}(t)$ is the additive noise.

The reconstructed time-course, $\hat{\boldsymbol{s}}(t,\boldsymbol{r}) = [\hat{s}_x(t,\boldsymbol{r}), \hat{s}_y(t,\boldsymbol{r}), \hat{s}_z(t,\boldsymbol{r})]^T$, for a given location $\boldsymbol{r}$ to the vector beamformer can be written as

$$\hat{\boldsymbol{s}}(t,\boldsymbol{r}) = \boldsymbol{W}^T(\boldsymbol{r})\boldsymbol{b}(t), \tag{2}$$

where $\boldsymbol{W}(\boldsymbol{r}) = [\boldsymbol{w}_x(\boldsymbol{r}), \boldsymbol{w}_y(\boldsymbol{r}), \boldsymbol{w}_z(\boldsymbol{r})]$ is a $M \times 3$ matrix of the vector beamformer coefficients. To obtain a tomographic map for all the brain locations (voxels) for a given EEG/MEG segment, the power for each voxel is calculated as

$$\begin{aligned} &\boldsymbol{p}_\xi(\boldsymbol{r}) = \boldsymbol{w}_\xi^T(\boldsymbol{r})\boldsymbol{C}\boldsymbol{w}_\xi(\boldsymbol{r}) = \langle \hat{s}_\xi(t,\boldsymbol{r})^2 \rangle, \\ &\xi \in x, y, z;\ \boldsymbol{r} \in \Omega, \end{aligned} \tag{3}$$

where $\langle ... \rangle$ is the ensemble average, and Ω is the different location on the scanning grid which covers the whole brain (source-space) $\boldsymbol{C}$ is the covariance matrix

$$\boldsymbol{C} = \langle \boldsymbol{b}(t)\boldsymbol{b}^T(t) \rangle. \tag{4}$$

III. Spatial filter algorithms

Beamforming is a popular technique for localization and signal reconstruction of the brain sources in EEG and MEG and has been successfully applied [4–6] and the relative performance of different beamformers have been evaluated [10–12]. The vector weight normalized minimum variance (WNMV) beamformer, also known as Borgiotti-Kaplan [5], was used to reconstruct brain sources at each voxel.

A. WNMV beamformer

The WNMV beamformer was chosen for this study mainly because it does not have a location bias while the well known linearly constrained minimum variance (LCMV) beamformer has been shown to have a location bias [10]. The weight matrix of the vector WNMV beamformer is

$$\boldsymbol{W}_{WNMV}(\boldsymbol{r}) = \frac{\boldsymbol{C}^{-1}\boldsymbol{L}(\boldsymbol{r})\boldsymbol{P}^{-1}(\boldsymbol{r})}{\sqrt{\boldsymbol{P}^{-1}(\boldsymbol{r})\boldsymbol{Q}(\boldsymbol{r})\boldsymbol{P}^{-1}(\boldsymbol{r})}} \tag{5}$$

where $\boldsymbol{P}(\boldsymbol{r})$ and $\boldsymbol{Q}(\boldsymbol{r})$ are

$$\begin{aligned} &\boldsymbol{P}(\boldsymbol{r}) = \boldsymbol{L}^T(\boldsymbol{r})\boldsymbol{C}^{-1}\boldsymbol{L}(\boldsymbol{r}) \qquad \text{and} \\ &\boldsymbol{Q}(\boldsymbol{r}) = \boldsymbol{L}^T(\boldsymbol{r})\boldsymbol{C}^{-2}\boldsymbol{L}(\boldsymbol{r}). \end{aligned} \tag{6}$$

B. source-space-ICA

The proposed source-space-ICA is based on application of ICA as a blind source separation technique on the reconstructed time-courses of all brain voxels via the vector WNMV beamformer. Since the reconstructed time-course for a given location is a mixture of source signals at that location and background activity, i.e., $\hat{\boldsymbol{s}}(t,\boldsymbol{r}) \neq \boldsymbol{s}(t,\boldsymbol{r})$, ICA can be applied to separate the statistically independent source signals. The matrix of reconstructed time-courses $\hat{\boldsymbol{S}} \in \Re^{(3N \times K)}$ for all N brain points on the scanning grid and time samples K is

$$\hat{\boldsymbol{S}} = \begin{pmatrix} \hat{s}_x(t_1,\boldsymbol{r}_1) & \hat{s}_x(t_2,\boldsymbol{r}_1) & \cdots & \hat{s}_x(t_K,\boldsymbol{r}_1) \\ \hat{s}_y(t_1,\boldsymbol{r}_1) & \hat{s}_y(t_2,\boldsymbol{r}_1) & \cdots & \hat{s}_y(t_K,\boldsymbol{r}_1) \\ \hat{s}_z(t_1,\boldsymbol{r}_1) & \hat{s}_z(t_2,\boldsymbol{r}_1) & \cdots & \hat{s}_z(t_K,\boldsymbol{r}_1) \\ \hat{s}_x(t_1,\boldsymbol{r}_2) & \hat{s}_x(t_2,\boldsymbol{r}_2) & \cdots & \hat{s}_x(t_K,\boldsymbol{r}_2) \\ \hat{s}_y(t_1,\boldsymbol{r}_2) & \hat{s}_y(t_2,\boldsymbol{r}_2) & \cdots & \hat{s}_y(t_K,\boldsymbol{r}_2) \\ \hat{s}_z(t_1,\boldsymbol{r}_2) & \hat{s}_z(t_2,\boldsymbol{r}_2) & \cdots & \hat{s}_z(t_K,\boldsymbol{r}_2) \\ \vdots & \vdots & \ddots & \vdots \\ \hat{s}_z(t_1,\boldsymbol{r}_N) & \hat{s}_z(t_2,\boldsymbol{r}_N) & \cdots & \hat{s}_z(t_K,\boldsymbol{r}_N) \end{pmatrix}. \tag{7}$$

The demixing equation by ICA is

$$\boldsymbol{H}^T\hat{\boldsymbol{S}} = \bar{\boldsymbol{S}}. \tag{8}$$

where

$$\boldsymbol{H} = [\boldsymbol{h}_1, \boldsymbol{h}_2, ..., \boldsymbol{h}_{3N}],\ \boldsymbol{H} \in \Re^{(3N \times 3N)}, \tag{9}$$

is the demixing matrix and each column of this matrix corresponds to the identified independent component in $\bar{\boldsymbol{S}}$,

$$\boldsymbol{h}_{ic} = \begin{pmatrix} h_{icx}(\boldsymbol{r}_1) \\ h_{icy}(\boldsymbol{r}_1) \\ h_{icz}(\boldsymbol{r}_1) \\ h_{icx}(\boldsymbol{r}_2) \\ h_{icy}(\boldsymbol{r}_2) \\ h_{icz}(\boldsymbol{r}_2) \\ \vdots \\ h_{icz}(\boldsymbol{r}_N) \end{pmatrix},\ ic = 1, 2, ..., 3N, \tag{10}$$

and each row of $\bar{\boldsymbol{S}}$ is an independent component,

$$\bar{\boldsymbol{S}} = \begin{pmatrix} \bar{s}_1(t_1) & \bar{s}_1(t_2) & \cdots & \bar{s}_1(t_K) \\ \bar{s}_2(t_1) & \bar{s}_2(t_2) & \cdots & \bar{s}_2(t_K) \\ \vdots & \vdots & \ddots & \vdots \\ \bar{s}_{3N}(t_1) & \bar{s}_{3N}(t_2) & \cdots & \bar{s}_{3N}(t_K) \end{pmatrix} = \begin{pmatrix} \bar{\boldsymbol{s}}_1(t) \\ \bar{\boldsymbol{s}}_2(t) \\ \vdots \\ \bar{\boldsymbol{s}}_{3N}(t) \end{pmatrix}. \tag{11}$$

The demixing weight vector $\boldsymbol{h}_{ic}$ has 3 coefficients for each candidate location $\boldsymbol{r}$, which shows the strength of the corresponding independent component in 3 orthogonal directions for that location. To obtain a single value for each location, which provides a tomographic map for identified components, the 3-orthogonal values are summed

$$\hat{\boldsymbol{h}}_{ic} = \begin{pmatrix} h_{ic}(\boldsymbol{r}_1) \\ h_{ic}(\boldsymbol{r}_2) \\ \vdots \\ h_{ic}(\boldsymbol{r}_N) \end{pmatrix},\ ic = 1, 2, ..., 3N, \tag{12}$$

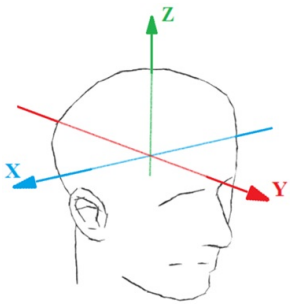

Fig. 1. The direction of the x, y, and z axes in the coordinate system used to describe the spatial location of the artificial dipole in the brain. Coordinate [0, 0, 0] is at the anterior commissure and in line with the anterior/posterior commissural line.

and

$$|h_{ic}(\boldsymbol{r}_n)| = \sqrt{h^2_{icx}(\boldsymbol{r}_n) + h^2_{icy}(\boldsymbol{r}_n) + h^2_{icz}(\boldsymbol{r}_n)}, \quad n = 1, 2, ..., N. \tag{13}$$

By projecting the weight vector $\hat{\boldsymbol{h}}_{ic}$ to the 3D scanning grid, it is possible to obtain the tomographic map of the corresponding independent components, $\bar{\boldsymbol{s}}_{ic}$.

As the number of reconstructed time-series is large ($3N$) depending on how many voxels were defined to scan the brain volume, it is desirable to apply principal component analysis (PCA) as a dimension-reduction technique to reduce the $\hat{\boldsymbol{S}}$ dimension before applying ICA. In this way the computational demand decreases considerably and, after running ICA, the dimension of $\bar{\boldsymbol{S}}$ and $\boldsymbol{H}$ will be $N' \times T$ and $3N \times N'$ respectively and N' is an arbitrary number such as 10, 50, or 100 which refers to the first N' principal components $\hat{\boldsymbol{S}}$ with highest variances and should be defined for PCA.

IV. Computer Simulations

To evaluate the performance of source-space-ICA, simulated EEG data were synthesized by equation 1 which contained three sources as shown in Fig. 2 and $\boldsymbol{\eta}(t)$ was real EEG. The real EEG was obtained from a healthy subject. The 64-channel 10-20 system was used for the location of EEG electrodes and the EEG was sampled at 250 Hz. MNI coordinates are used to describe the locations in the brain. The boundary element method (BEM) model of the head [13], obtained from the average MNI-template brain and implemented via the FieldTrip toolbox [14], was used to calculate the lead-field matrix. The x, y, and z axes are shown in Fig. 1. The length of the simulated EEG was 6 s. The EEGLAB toolbox [15] was used for ICA and PCA algorithms. The PCA algorithm reduced the dimension of the signal matrix $\hat{\boldsymbol{S}}$ to the first 30 principal components.

The SNR of the three brain sources superimposed on the real EEG was defined as the Frobenius norm of the source signal matrix to that of the real EEG matrix. The location of the three sources is shown in Fig. 2 and their normalized time-courses in Fig. 3. A 3D grid, with approximately 1200 locations which covers the whole brain, was used for scanning the brain with the beamformer.

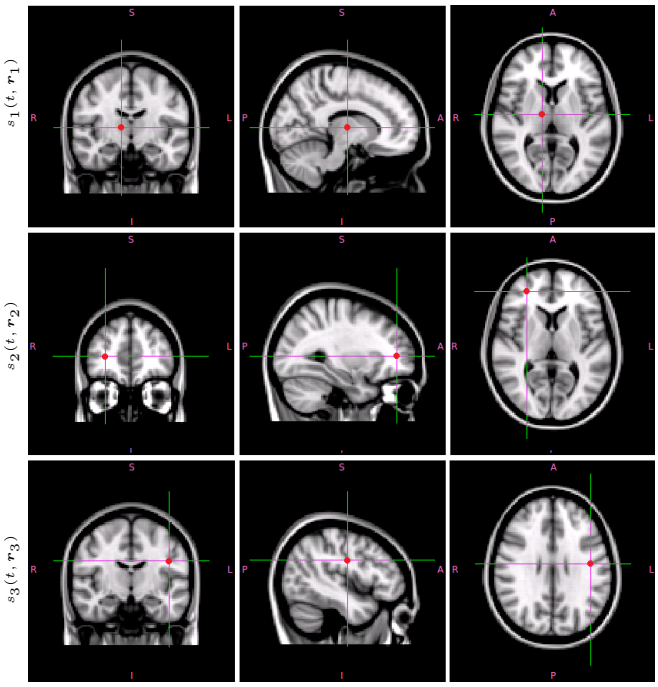

Fig. 2. The red dot shows the spatial location of the three sources on an MNI head. The location of the three sources is: $\boldsymbol{r}_1$ =[12, -12, 6]^T mm, $\boldsymbol{r}_2$ =[30, 46, 6]^T mm, and $\boldsymbol{r}_3$ =[-44, -12, 28]^T mm for s_1, s_2 and s_3 respectively. The orientations of these sources are: $\|\boldsymbol{q}(\boldsymbol{r}_1)\|$ =[0, 0, 1]^T, $\|\boldsymbol{q}(\boldsymbol{r}_2)\|$ =[0.57, 0.57, 0.57]^T, and $\|\boldsymbol{q}(\boldsymbol{r}_3)\|$ =[0, 1, 0]^T.

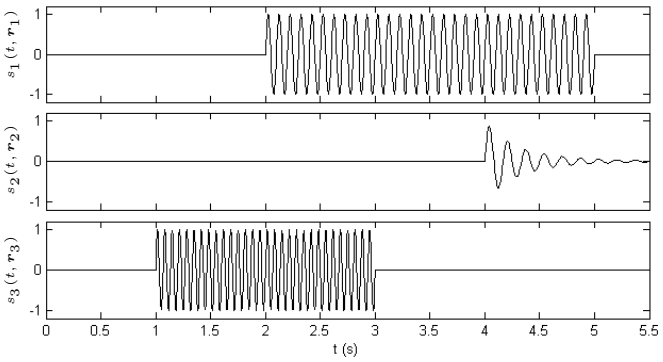

Fig. 3. The time-courses of three simulated sources s_1, s_2, and s_3. s_1 and s_3 are sinusoidal at 10 and 15 Hz and s_2 is a damped 6 Hz sinusoid. The SNR of the three sources are 0.40, 0.25, and 1.00 respectively.

V. Results

Fig. 4 shows the time-courses of the first 9 (of 30) brain source signals found by source-space-ICA. By visual inspection, it is clear that components 1, 3, and 8 are the three sources, s_1, s_2 and s_3 respectively, superimposed on the real EEG. By projecting their corresponding demixing weights (equation 12) onto the scanning grid it is possible to localize these sources in the head (Fig. 5). The cross-hairs in Fig. 5 show the locations of the artificial sources (as shown in Fig. 2). For each component map, the centre of the voxel with the largest value was considered to be the location of the dipole for that component. The localization errors for sources s_1, s_2, and s_3 were calculated to be 11.5 mm, 2.8 mm and 7.2 mm.

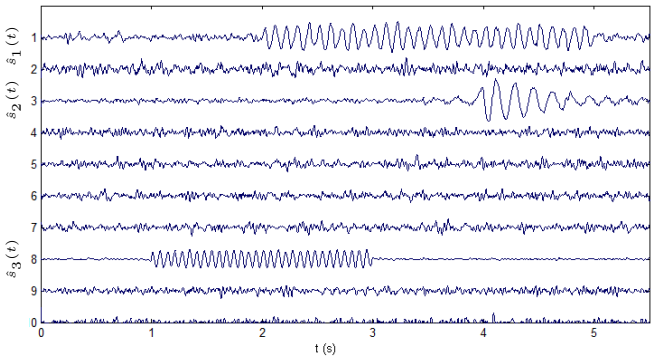

Fig. 4. The reconstructed time-courses of brain sources by source-space-ICA for a 6-s EEG segment. Components 1, 3, and 8 ($\bar{s}_1, \bar{s}_3$, and $\bar{s}_8$) represent s_1, s_2, and s_3 respectively.

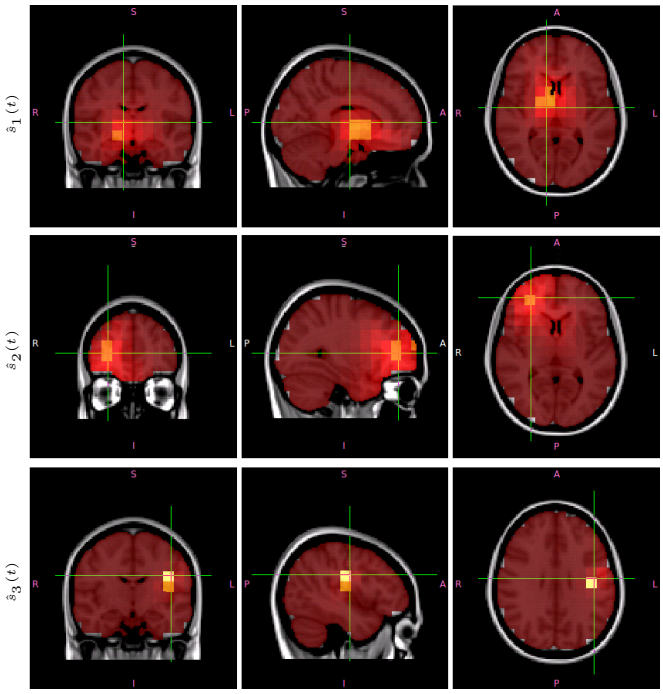

Fig. 5. Spatial location of the $\bar{s}_1, \bar{s}_3$, and $\bar{s}_8$ sources shown in Fig. 4. The cross-hairs show the actual location of the sources.

VI. Discussion

We have introduced a novel source-space-ICA approach to localization and time-course reconstruction of brain sources. The source-space-ICA successfully identified weak and deep sources, as well as a shallow source with a high SNR. The source-space-ICA applies the weight normalized minimum variance beamformer to reconstruct the brain oscillations for every point in the head. The ICA then separates different sources from each other, so that it is possible to identify weak brain sources. Although the localization error was 11.5 mm for s_1, the accuracy of source localization by source-space-ICA can be increased by band-pass filtering the source-space signal matrix to pass only the desired frequencies, this eases the task of ICA decomposing the signal mixtures. Another way is to apply a scanning grid with smaller voxels (in this study the size of each voxel was 12 mm^3). However, increasing the number of voxels will increase the computational effort.

The main difference between the source-space-ICA approach and other popular source localization methods, such as minimum variance beamformers and sLORETA, is that source-space-ICA identifies the sources based on their statistical independence, while other methods find the sources by measuring the magnitude of the sources in different brain locations. This means that only sources stronger than the background signal can be identified. Although ICA was applied for localization of brain sources in [9], their approach utilizes dipole fitting for ICA components. A major limitation of this is with respect to localization of cluster sources, as it can only find a single point source for every identified component. In addition, in this approach, ICA is applied to scalp signal only, while in source-space-ICA the ICA is applied to the estimated signals of all brain voxels.

References

[1] J. Sarvas, "Basic mathematical and electromagnetic concepts of the biomagnetic inverse problem," *Phys. Med. Biol*, vol. 32, pp. 11–22, 1987.

[2] M. S. Hamalainen and R. J. Ilmoniemi, "Interpreting magnetic fields of the brain: minimum norm estimates," *Med. Biol. Eng. Comput.*, vol. 32, pp. 35–42, 1994.

[3] R. D. Pascual-Marqui, "Standardized low-resolution brain electromagnetic tomography (sLORETA): technical details," *Methods Find. Exp. Clin. Pharmacol.*, vol. 24 Suppl D, pp. 5–12, 2002.

[4] B. D. Van Veen, W. van Drongelen, M. Yuchtman, and A. Suzuki, "Localization of brain electrical activity via linearly constrained minimum variance spatial filtering," *IEEE Trans. Biomed. Eng.*, vol. 44, no. 9, pp. 867–880, 1997.

[5] K. Sekihara, S. S. Nagarajan, D. Poeppel, A. Marantz, and Y. Miyashita, "Reconstructing spatio-temporal activities of neural sources using an MEG vector beamformer technique," *IEEE Trans. Biomed. Eng.*, vol. 48, no. 7, pp. 760–771, 2001.

[6] S. Robinson and J. Vrba, "Functional neuroimaging by synthetic aperture magnetometry (SAM)," in *Proc. 11th Int. Conf. Biomagnetism.*, T. Yoshimoto, M. Kotani, S. Kuriki, H. Karibe, and N. Nakasato, Eds. Sendai: Tohoku Univ. Press, 1999, pp. 302–305.

[7] K. Sekihara, M. Sahani, and S. S. Nagarajan, "Localization bias and spatial resolution of adaptive and non-adaptive spatial filters for MEG source reconstruction," *NeuroImage*, vol. 25, pp. 1056–1067, 2005.

[8] S. Sanei and J. A. Chambers, *EEG signal processing*. Chichester, West Sussex: John Wiley & Sons, LTD, 2007.

[9] S. Makeig, S. Debener, J. Onton, and A. Delorme, "Mining event-related brain dynamics," *Trends Cogn. Sci.*, vol. 8, pp. 204–210, 2004.

[10] R. E. Greenblatt, A. Ossadtchi, and M. E. Pflieger, "Local linear estimators for the linear bioelectromagnetic inverse problem," *IEEE Trans. Biomed. Eng.*, vol. 53, no. 9, pp. 3403–3412, 2005.

[11] M. X. Huang, J. J. Shih, R. R. Lee, D. L. Harrington, R. J. Thoma, M. P. Weisend, F. Hanlon, K. M. Paulson, T. Li, K. Martin, G. A. Millers, and J. M. Canive, "Commonalities and differences among vectorized beamformers in electromagnetic source imaging," *Brain Topogr.*, vol. 16, no. 3, pp. 139–158, 2004.

[12] Y. J. Mohamadi, G. Poudel, C. Innes, and R. Jones, "Performance of beamformers on EEG source reconstruction," *Proc. Int. Conf. IEEE Eng. Med. Biol. Soc.*, vol. 34, pp. 2517–2521, 2012.

[13] T. F. Oostendorp and A. van Oosterom, "Source parameter estimation in inhomogeneous volume conductors of arbitrary shape," *IEEE Trans. Biomed. Eng.*, vol. 36, pp. 382–391, 1989.

[14] R. Oostenveld, P. Fries, E. Maris, and J. M. Schoffelen, "Fieldtrip: Open source software for advanced analysis of MEG, EEG, and invasive electrophysiological data," *Comput. Intell. Neurosci.*, vol. 2011, pp. 1–9, 2011.

[15] A. Delorme and S. Makeig, "EEGLAB: an open source toolbox for analysis of single-trial EEG dynamics," *J. Neurosci. Methods*, vol. 134, pp. 9–21, 2004.